

# A STUDY OF WHIPLASH INJURY OCCURRENCE MECHANISMS USING HUMAN FINITE ELEMENT MODEL

**Junji Hasegawa**

Toyota Motor Corporation, Japan

**Akiyoshi Shiomi**

Toyota Communication Systems Co., LTD., Japan

Paper Number 195

## 1. Abstract

Approximately 20% of car-to-car accidents in the U.S. are believed to be rear-end collisions, and approximately 10% of the whiplash injuries resulting from rear-end impacts require longer term therapy. Thus, the societal cost of whiplash injuries is a common problem worldwide, so its prevention is a hot topic globally. However, whiplash injuries involve a very wide range of symptoms, such as surgical symptoms, neurological symptoms, audiological symptoms, otorhinolaryngological symptoms, sense-of-balance symptoms, teeth-occlusion symptoms, etc. Whiplash injuries have such subtle characteristics that patients themselves complain of various symptoms in addition to these diverse symptoms, even in the absence of objective medical evidence, at times.

We have developed an AM 50%-tile finite-element model of the whole human body, called THUMS (Total Human Model for Safety), to study the mechanisms of human-body injury during a collision. In this research, the same model was utilized to study the mechanisms of injury to the cervical vertebrae region from whiplash during a collision. We developed a cervical spine model that newly incorporates spinal cord, nerve roots, cerebrospinal fluid (CSF), spinal dura mater, etc., and then verified the accuracy of this model by means of cadaver test data. Its validity was examined on the basis of various hypotheses studied to date: the myalgia hypothesis, the theory of nerve-root pressure caused by compression of the spinal cord and nerve roots, the theory of facet joint impingement, the theory of the shear deformation of facet joints and ligaments, etc. Also, whiplash symptoms resulting from the leakage of CSF (i.e., the low intracranial pressure syndrome), which recently has attracted attention in Japan, also are evaluated with respect to the existence of spinal dura mater spinalis injury.

## 2. Introduction

Japan also has many whiplash accidents. Figure 1 shows the proportions of the number of persons by injury locations in all accidents, based on Ref. [1] regarding insurance payouts during the year from April 2000 to March 2001 in Japan. With approximately 520,000 cases, the neck was the most common injury location, accounting for approximately 45% of the all accidents. The approximately 440,000 victims of car-to-car rear-end accidents accounted for at least one-third of all victims, the overwhelming majority (i.e., 340,000) of whom were victims of neck injuries in rear-end collisions.

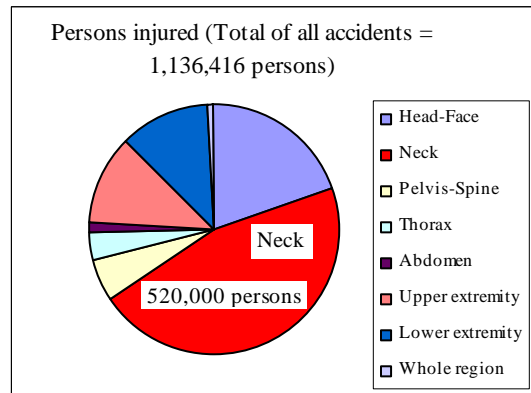


**Figure 1 Number of Victims in All Accidents, by Injury Location [1]**

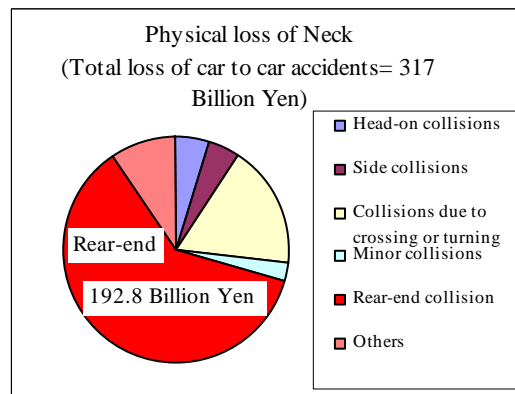


**Figure 2 Neck Injury Losses by All Car-to-Car Accidents [1]**

Also, Figure 2 shows the proportions of losses resulting from neck injuries of rear-end collisions in all car-to-car accidents. It is evident from the figure that they were highest at ¥192.8 billion and accounted for 60% of all car-to-car accidents and 14.5% of the all accidents. In Japan, as elsewhere, reduction of whiplash injuries is a major challenge. In addition, the term “whiplash injuries” in this paper means the whiplash associated disorders (WAD) defined by the Quebec Task Force [2] in 1995.

## 3. Anatomical Cervical Spine

### 3-1. Vertebral Body and Ligament [3], [4]

Figure 3 shows the atlas (C1) and the axis (C2), which is the upper cervical vertebrae, as well as the third cervical vertebra (C3) and those below it, which are the similarly shaped lower cervical vertebrae. At

each vertebral body, the cancellous bone is surrounded by thin and hard cortical bone. Upper and lower vertebral bodies are connected by the intervertebral disc of fibrocartilage. To control the movement of the cervical vertebrae within their physiological ranges, the vertebral bodies are surrounded by the anterior longitudinal ligament (ALL), the posterior longitudinal ligament (PLL), the articular capsule of the joint between articular processes, the ligamentum flavum (LF), the interspinous ligament (ITL), the supraspinous ligaments (SSL), intertransverse ligament (ISL), and other ligaments, as shown in Figure 3.

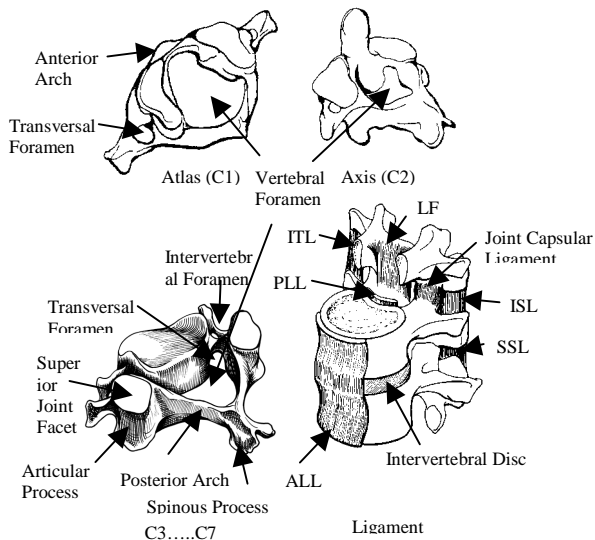


**Figure 3 Cervical Vertebrae and Ligaments [3],[4]**

### 3-2. Spinal Cord and Dura Mater [5]

The spinal cord is in the spinal canal within the vertebral foramen surrounded by the vertebrae. As shown in Figure 4, the spinal cord itself is protected by the pia mater, the dentate ligament, the subdural space and subarachnoid space filled with CSF, and the dura mater. The colorless, transparent CSF is produced by the choroid plexus of the cerebral ventricle, circulates within the cerebrospinal subarachnoid space, and is absorbed in the brain's superior sagittal sinus. It is said that, in a healthy adult, the capacity is approximately 150 ml and the daily production is approximately 500 ml. The low intracranial pressure syndrome, which recently has attracted attention in Japan, is caused by the leakage of CSF from the dura mater, which decreases the amount of spinal fluid and lowers the intracranial pressure. As a result, the brain cannot float in spinal fluid, so the brain drops downward. This is believed to intensify symptoms such as headache, nausea, vertigo, lassitude, and back and neck pain. Eight pairs of cervical nerves go out of the cervical region.

### 3-3. Nerves [3]

The nerve roots that exit from the spinal cord pass through the dura mater and then through each

intervertebral foramen at each level of the vertebral body, for which they go out of the spinal canal.

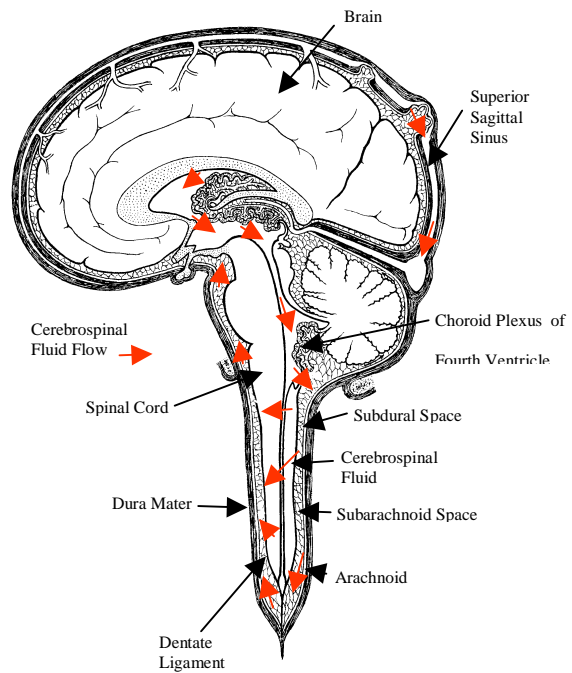


**Figure 4 Meninges to Brain, Spinal Cord and Cerebrospinal Fluid [5]**

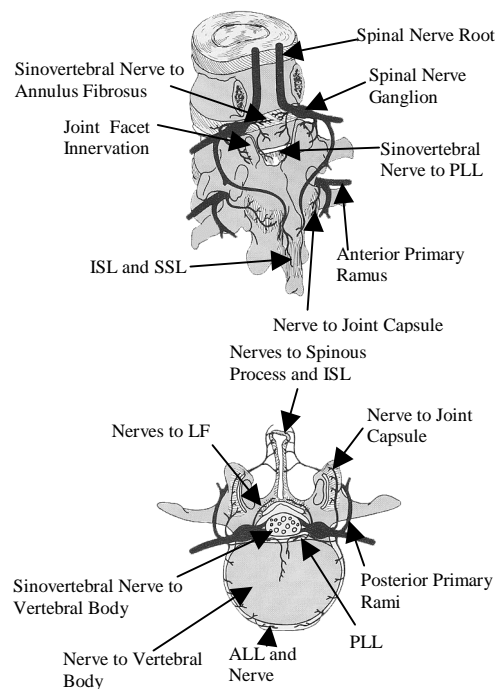


**Figure 5 Sensory Innervation of Nerve in Spine [3]**

As a result, these nerve roots are affected by spinal displacement or trauma. Figure 5 shows the structure of the sensory innervation of the spine. The nerves resulting from the sinus-vertebral artery nerves are distributed in the posterior annulus fibrosus and the PLL. Capsular structures also have sensory nerves, and bone structures are controlled via the autonomic nervous system. The paraspinous muscles also have sensory nervous system. It is believed that any physical,

chemical or emotional, psychological stimulation will result in nerve-root pain.

### 3-4. Cervical Vertebral Artery [6]

The vertebral artery passes from cervical vertebra C1 to C6 and through the transverse foramen. So, deformation of a cervical vertebra as the result of its hyperflexion-extension or suddenly turning around sometimes exerts pressure on the artery, which causes vertigo, fainting, etc. Pressure on the vertebral artery stimulates the sympathetic nerves surrounding it, thereby causing headache, nausea, tinnitus, facial pain and flushing, pharyngeal sensory abnormality, etc.

### 4. Mechanisms for the Occurrence of Whiplash Injury

King [7] summarized the whiplash theories to date and listed the main ones as follows:

- I: One hypothesis is that whiplash injuries are caused by severe hyperextension such that the head's extension angle exceeds 90°. This was the initial theory. Later, the introduction of the headrest failed to prevent whiplash injuries perfectly, so other hypotheses were proposed.
- II: In another one, pain is caused [8] by the spinal nerves or the dorsal roots as the result of increased pressure in the spinal canal and the cervical region during extension in whiplash. Static and dynamic pulling tests of the cervical region were performed using pigs. It was reported that, in the static pull test, no abnormality was observed in the nerve roots of the cervical region; in the dynamic test, however, abnormality was observed in nociceptive nerve plexus, by means of variation in the pressure within the spinal canal, based on S-shaped deformation of the cervical region. In the following equation (1), the predicted pressure (Pa) at the C4 vertebra level was estimated based on hydraulic theory on CSF flow and from the experimental values.

$$P_a = 1100 * [0.1 * A_{rel} + \left(\frac{1}{2}\right) * (V_{rel})^2] \quad (1)$$

The Neck Injury Criteria (NIC) [9] was proposed as criteria for evaluating cervical region injuries.

$$NIC = A_{rel} * L + (V_{rel})^2 \quad (2)$$

Here, L is the length parameter, Arel is the relative acceleration between the head and 1st thoracic vertebra T1, and Vrel is their relative velocity in the same way.

- III: Hypothesis based on facet joint surface impingement between upper and lower vertebrae [10]

During a rear-end collision, shear forces and axial compressive forces are exerted on the cervical

vertebrae. According to this hypothesis, the center of rotation by extension during whiplash moves upward, so facet joint injury occurs as the result of the facet joint impingement when the lower articular process of the upper cervical vertebra contacts the upper articular process of the lower cervical vertebra. Also, cervical-region pain occurs as the result of the inflammation that occurs after the synovial folds with the articular capsule of the joint are stimulated by the facet joint impingement.

- IV: Hypothesis based on the shear deformation of the capsules that covers the facet joint

In this hypothesis, the compressive loading of the cervical vertebrae as the result of the straightening of the thoracic spinal column by the contact to seat during a rear-end collision causes the cervical vertebrae to slide relative to each other, thereby stretching the joint capsule which results in inflammation and pain.

### 5. Summary of the Head-to-Cervical Spine Model

To evaluate and study various whiplash-injury mechanisms in this study, we developed a model of the head-to-cervical complex, shown in Figure 6, based on the THUMS whole-body model. The spinal cord, CSF, nerves, cervical artery, etc., was newly added to enable the evaluation of various whiplash injuries. To measure the CSF pressure, which is the basis of NIC, the pia mater, dura mater, and spinal fluid surrounding the spinal cord also were modeled. For the nerves, the average cross-sectional area of the nerve roots is extremely small (i.e., approximately 1.2 mm<sup>2</sup>), so the time steps for calculation were taken into consideration to model with bar elements.

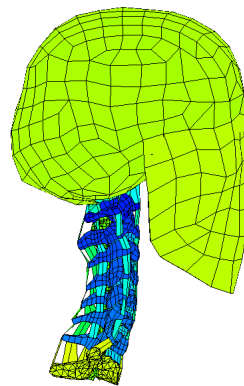


**Figure 6 Head to Cervical Spine Complex Model**

Also, the main phenomenon with whiplash generally occurs within 200 ms during rear-end collisions. It was reported [11] that, when passengers are subjected to rear-end collisions unexpectedly in traffic accidents, at least 200 ms are required to reflexively activate the muscles, so muscle function is minimal during a whiplash. In this study, therefore, the whiplash injury mechanism was analyzed without a muscle model. Furthermore, for details of the head and cervical region model, refer to Appendix I.

## 6. Verification of the Cervical Spine Model

Before whiplash injury was verified by means of a head-to-cervical spine model, the flexion–extension characteristics, which are especially important in the whiplash phenomenon, were verified at the vertebra level. As mentioned previously, there is considerable anatomical difference of their shapes between upper cervical vertebra and lower cervical vertebra. As a result, the flexion–extension behavior of the lower cervical vertebra and the upper cervical vertebra was verified individually.

### 6-1. Cervical Vertebrae Unit

#### (I) Flexion–Extension Behavior of the Lower Cervical Vertebra [4, 12]

Because the lower cervical vertebrae have similar shapes, the C4-C5 cervical-vertebrae complex was selected as the representative lower cervical vertebrae in this study. The material properties and types of soft tissues vary. Therefore, many hours are required to verify the behavior of the human-body model. The material properties of the ligaments, membranes, and fibers of such cervical-vertebrae regions were identified by using iSIGHT, general-purpose software for optimization. Figure 7 shows a comparison between simulation and experimental result on the bending moment vs. the rotation angle characteristics in the flexion-extension.

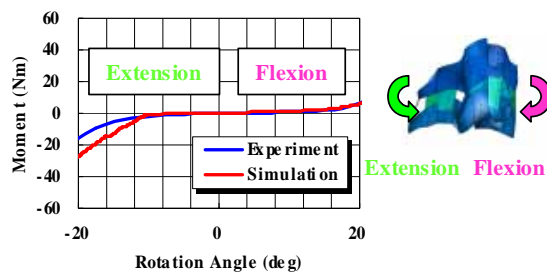


**Figure 7 Flexion-Extension Characteristics at C4-C5 level**

The abrupt rise in the extensional moment results from the contact between the lamina of vertebral arch of adjacent cervical vertebrae. The qualitative trends on simulation result agree well with the tests. This procedure was found to be effective in identifying material properties, so the same method also was applied to the C1–C2 upper cervical vertebrae, where the types, shapes, and functions of ligaments differ significantly from those of the lower cervical vertebrae.

#### (II) Flexion–Extension Behavior of the Upper Cervical Vertebrae [13]

As the verification data, the material properties were identified by means of the experimental data [13] obtained by using the head-to-C2 specimen of a human body. Figure 8 shows a comparison of the moment vs. rotation angle during the flexion–extension of the head-to-C2 region. As in the case

of the lower cervical vertebrae, it is evident that they agree well.

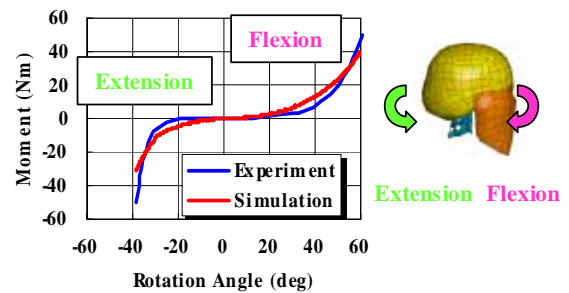


**Figure 8 Flexion-Extension Characteristics at Head-C2 level**

### 6-2. Verification of the Head-to-Cervical Spine Complex Model [11]

The behavior during whiplash extension will be verified next, based on the experimental data obtained by using the cervical spine specimen of a human cadaver, as shown in Figure 9.

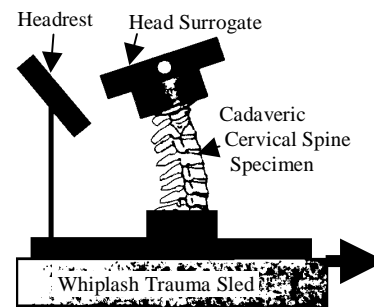


**Figure 9 Schematic Diagram of the Whiplash Apparatus in Ref. [11]**

As in the case of the head-to-cervical spine model, this specimen was composed of the head to T1, and except for the ligaments around the cervical vertebrae, the soft tissues including muscles were removed. Also, substitutes for the headrest and the human head, such as those shown in Figure 9, were used in place of the cadaver and real headrest. T1 was anchored to the sled by means of a resin mount. Also, the peak acceleration level applied on the sled was varied from 2.5 to 10.5 G. For the following two reasons, we decided to analyze up to the moment in time when the head contacts the headrest.

- The aim of the whiplash trauma test in Ref. [11] is to target the behavior of the cervical vertebrae until the head substitute collides with the headrest.
- Details such as the placement of the test device, dimensional conditions, headrest characteristics, etc., are unknown.

The initial distance from the occiput to the headrest was set to 10 cm, on average [14]. The mass of the

head model was approximately 4.5 kg, and the inertial moment around the y-axis was 0.0184 kg·m<sup>2</sup>. In this analysis, a rigid-body model was used for the head. Also, in this analysis a peak acceleration of 10.5 G was used as a sled condition. Figures 10 and 11 shows the simulation results, which are the head's horizontal relative displacement at head center-of-gravity position and its rotational angle during extension up to 60 ms as well as a comparison of the experimental results.

As is evident from Figure 11, at approximately 60 ms the head's horizontal relative movement distance reached 10 cm, at which time the head began to contact the headrest. It is obvious that the experiment and simulation trends agree well.

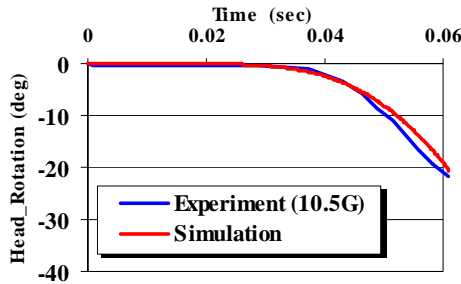


Figure 10 Head Rotational Angle-Time History

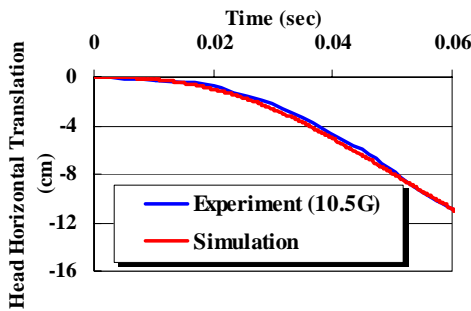


Figure 11 Head Horizontal Displacement-Time History

### 6-3. Discussion of Cervical Spine Behavior

Figure 12 shows the behavior from the head to the cervical region. Figure 13 is a diagram of the rotational angle-time histories of each part of the cervical vertebrae. It was observed that the head hardly moved until 30 ms, after which the cervical vertebrae deformed into an S-shape (heavy red line in Fig. 12) as a result of the horizontal movement of the sled, that is T1. As aforementioned, 60 ms was the instant when the head contacted the headrest.

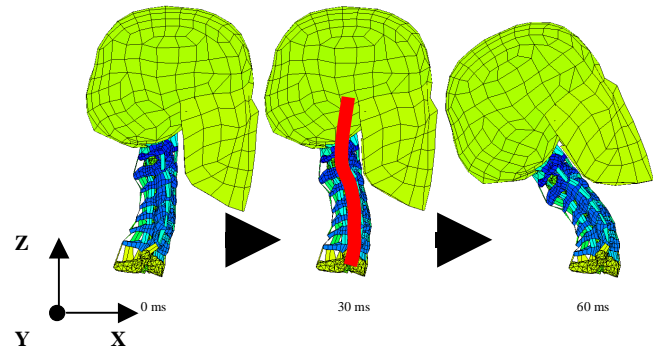


Figure 12 Head and Neck Responses during Whiplash

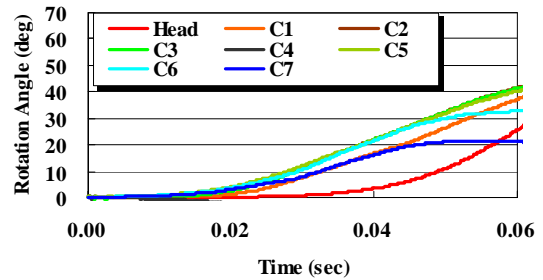


Figure 13 Rotational Angle-Time History of Each Cervical Vertebrae including Head

It was possible to reproduce the S-shaped deformation of the cervical vertebrae, which appear at the initial stage of the whiplash phenomenon, so we studied in further detail the analytical results for each part of the cervical vertebrae.

Figure 14 shows the relative rotational angles which mean the angles of the upper vertebra relative to the neighboring lower vertebra. In this whiplash phenomenon, the upper cervical vertebrae including head are flexed, while C5-C7 vertebrae are extended.

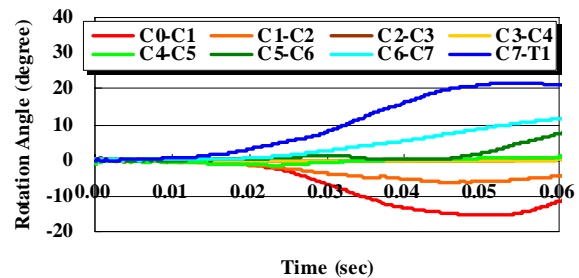


Figure 14 Relative Rotational Angle-Time History

Figure 15 shows the resultant force-time histories on the facing facet joints on the right side. There is no modeling of joint cartilage in this model. From this figure, it is evident that, immediately after a whiplash, opposing superior and inferior joint surfaces impinge, producing impact loading. The observed trends were for the loading of the C1-C2 facet joint to increase in the first half due to the initial flexion, while for the

loading of the C6-C7 joint to increase in the second half due to extension from the beginning.

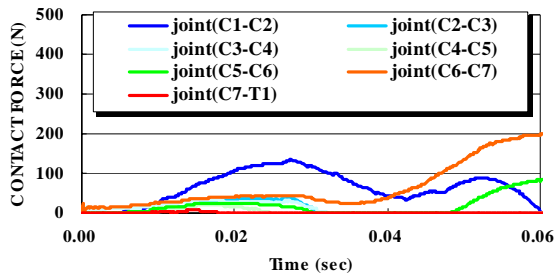


Figure 15 Contact Forces on Each Facet Joints

Also, Figure 16 shows a history of the moment about Y-axis, axial (Z-axis), and shear (X-axis) force in the upper cervical region.

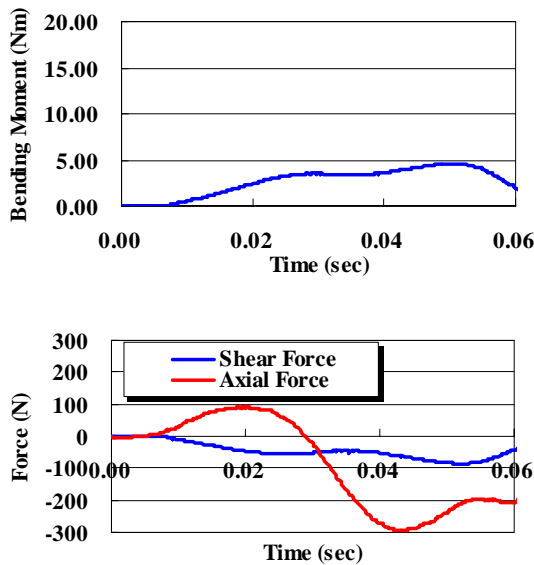


Figure16 Bending Moment, Shear and Axial Force of Upper Cervical Region

Also, Figure 17 shows the relative displacements between C4 and C5 facet joints. As an example, “Anterior Disp-X” in this figure means the displacement in X-direction at anterior sites in the inferior surface of C4 joint and the superior surface of C5 joint.

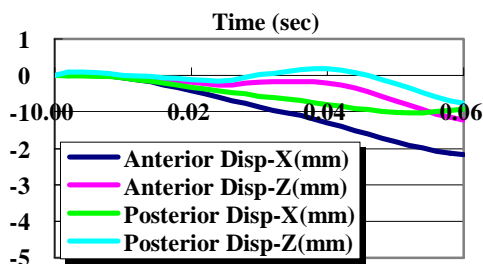


Figure 17 Relative Displacements at the Location of C4-C5 Facet Joint

Up to 60 ms, the maximum relative displacement in the anterior site was approximately 2 and 1 mm in x- and z-directions, respectively. Also, their displacement in the posterior one was approximately 1 and 0.8 mm in the x- and z-directions, respectively.

Their peak displacements are nearly same to the experimental results reported by Yoganandan et al. [15]. They used human cadaver head-neck complexes with skins and musculature intact and took vertebrae’s behavior during whiplash by high-speed video camera. Also, when developing the NIC criteria, Svensson et al. [8] measured the CSF and intracranial pressures in pig and human-cadaver tests. Similarly, we too predicted the CSF pressure by using our model. Figure 18 shows the pressure–time curve of the CSF during that time.

To simulate the hydrodynamic responses of the CSF, analysis was performed based on the Murnaghan equation of state [16], in which the compressibility is increased artificially. The predicted results were on the same order as the CSF pressure values in the whiplash experiments with cadavers [17], but it seems that the profile is different from the experimental one, though they couldn’t be compared each other under same condition.

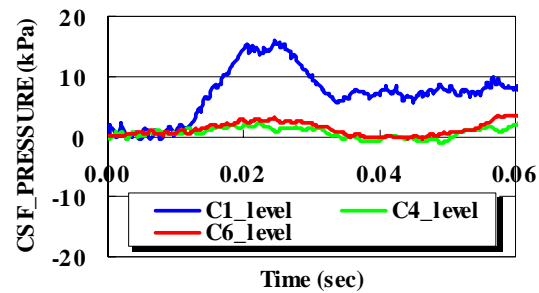


Figure 18 Pressure-Time History of CSF

#### 6-4. Evaluation of Whiplash Injuries

The validity of this model was verifiable, so we checked the analytical results by means of the injury criteria as well as the injury check items based on whiplash injury hypotheses proposed to date. As mentioned previously, in the head-to-cervical spine complex specimen tests used for verification, the headrest was set so that the head did not extend beyond its physiological ranges, thereby minimizing neck injury. Also, the same paper [11] makes no mention of an injured area or the presence or absence on whiplash injuries, so it was determined that there is no injury to the cervical vertebrae under a 10.5 G sled condition. The injury evaluation results yielded by our head-to-cervical spine model are tabulated in Table 1. Also, the principal disorders are explained.

Table 1 Prediction of Cervical Injuries during 10.5G Whiplash Trauma

○ no injuries   - indefinite   × injuries

Check items for injuries	Judgment
Strain on Vertebral Bone	○





## 8. Conclusions

- (1) A cervical spine model that enables the evaluation of a wide range of whiplash symptoms was developed and validated.
- (2) The results of whiplash injury predictions based on the vehicle acceleration data during real rear-end-collision accidents were reasonable, and they proved to be applicable also to the prediction of various whiplash injuries.
- (3) It was found that the human body FE model is an effective tool for analyzing new injury mechanisms and can contribute significantly to the development of injury-evaluation techniques, such as the suggestions for real dummy improvements and the guidelines of injury criteria based on the injury occurrence mechanism and so on, with experimental tests in the future.

## 9. Future Plans

We plan to incorporate the cervical spine model developed in this study into the whole human body model and to perform whiplash analyses using the full-scale car model, as shown in Figure 25.

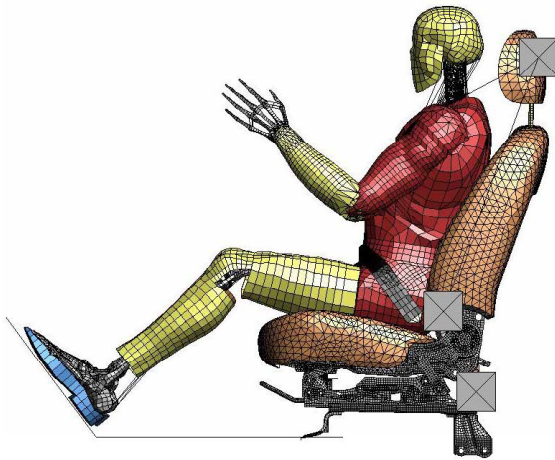


**Figure 25 Whiplash Analysis of Whole Human Model with Full Seat Model**

At present, the analysis of a human-body model requires considerable time, even when a supercomputer is used. Feeding back the study results obtained by means of the human body model to test dummy construction and evaluation criteria could possibly have future vehicle development application.

This research targeted whiplash. In the future, however, we would like to apply the human-body model to further research of other injury mechanisms. Furthermore, we would like to apply it in a wide range of other fields, not merely the field of automobile collisions.

For that purpose, we will need to supplement the efforts of our own automobile engineers by increasing collaboration with the research organizations of manufacturers, universities, etc., in a wide range of

disciplines (e.g., medicine, engineering, accident investigation).

## 10. Acknowledgements

For their assistance with this analysis we would like to thank the parties concerned at Toyota Central R&D Labs, Inc., especially Ms. Kato. We also would like to thank Dr. Hsu of Engineous Japan Inc., Dr. Cholewicki of Yale University, and Dr. A. Eichberger (University of Technology, Graz) for their advice.

## References

- [1] The Marine & Fire Insurance Association of Japan, Inc., "2002 traffic accident survey from automobile insurance payment data: the number of bodily injuries and property damage accidents, and the sum of economic loss", <http://www.sonpo.or.jp/> Japan, 2002
- [2] W. O. Spitzer, et al., "Scientific monograph of the Quebec task force on whiplash-associated disorders", Spine [Suppl]:20, 1995.
- [3] A. A. White III, M. M. Panjabi, 1990, "Clinical biomechanics of the spine", 2<sup>nd</sup> Ed., Lippincott Williams & Wilkins, Philadelphia.
- [4] Marko de Jager, "Mathematical head-neck models for acceleration impacts", Thesis Technische Universiteit Eindhoven, pp.42-47, 1996
- [5] U. Kaneko, 1982, "Nippon Human Anatomy, Vol. III Angiologia, Systema Nervosum", Nanzando Company, Limited, Tokyo, Japan
- [6] K. Nibu, et al., "Dynamic elongation of the vertebral artery during an in vitro whiplash simulation", Eur Spine J., Vol. 6, pp.286-289, 1997
- [7] A. I. King, 1999, "What is a reasonable hypothesis for the cause of whiplash associated disorders?" SAE TOPTEC, Costa Mesa, California
- [8] M. Y. Svensson et al., 1993, "Pressure Effects in the Spinal Canal during Whiplash Extension Motion- A Possible Cause of Injury to the Cervical Spinal Ganglia, IRCOBI, pp.189-200
- [9] O. Bostrom et al. (1996 "A New Neck Injury Criterion Candidate-Based on Injury Findings in the Cervical Spinal Ganglia after Experimental Neck Extension Trauma", IRCOBI, pp.123-136
- [10] K. Kaneoka., et al, 1998, "The Mechanism of Whiplash Injury" 1998.10.23-24, Proceedings of 2<sup>nd</sup> Toyota Human Life Support Biomechanics Symposium, pp.45-50
- [11] Jacek Cholewicki, et al., "Head kinematics during in vitro whiplash simulation", Accid. Anal. and Prev., Vol.30, No.4, pp.469-479, 1998
- [12] M. M. Panjabi., et al., 1994, "On the understanding of clinical instability", Spine, Vol. 19, No. 23, pp.2642-2650
- [13] R. W. Nightingale, et al., 2002, "Comparative strengths and structural properties of the upper and lower cervical spine in flexion and extension", Journal of Biomechanis, Vol.35, pp.725-732

[14] R. Minton, et al., 1997, "Causative Factors in whiplash injury: Implications for current seat and head restraint design", IRCOBI, pp.207-222

[15] N. Yoganandan, et al., 1998, "Cervical Spine Vertebral and Facet Joint Kinematics under Whiplash", Journal of Biomechanical Engineering, Vol. 120, pp.305-307.

[16] Pam-Crash Ver.2000 Solver Notes Manual

[17] A. Eichberger, et al., 2000, "Pressure measurements in the spinal canal of post-mortem human subjects during rear-end collision and correlation of results to the neck injury criterion", Accident Analysis & Prevention, Vol. 32, pp.251-260

[18] R. U. Repo., et al., 1977, "Survival of articular cartilage after controlled impact", Journal of bone and joint surgery, Vol.59-A, No.8, pp.1068-1075

[19] A. Nygren, et al., 1985, "Effects of different types of headrests in rear-end collisions", 10<sup>th</sup> ESV Conference, pp.85-90

[20] M. Krafft, et al., 2000, "How crash severity in rear impacts influences short- and long-term consequences to the neck", Accident Analysis & Prevention, Vol. 32, pp.187-195

[21] Viewpoint Premier Catalog, 2000 edition  
<http://www.viewpoint.com>

[22] N. Yoganandan, et al., 1998, "Biomechanical assessment of human cervical spine ligaments", SAE #983159

[23] H. Yamada, 1970, "Strength of biological materials", Williams & Wilkins Company, Baltimore

[24] S. C. Cowin, 1991, "Bone Mechanics", CRC Press, Inc., Florida

## Appendix I The description of cervical spine model

We constructed new models such as spinal cord, dura mater, CSF and so on, based on the human geometrical data of Viewpoint Digital™ and incorporated them into the existing cervical model of THUMS. And we analyzed by using Software "Pam-Crash". Figure 26 shows the disassembled diagram of the cervical spine model.

- (a) Head-Cervical Spine Complex Model
- (b) Global View of Cervical Spine
- (c) Visualization of Vertebral Canal
- (d) Cross-section at C7 level

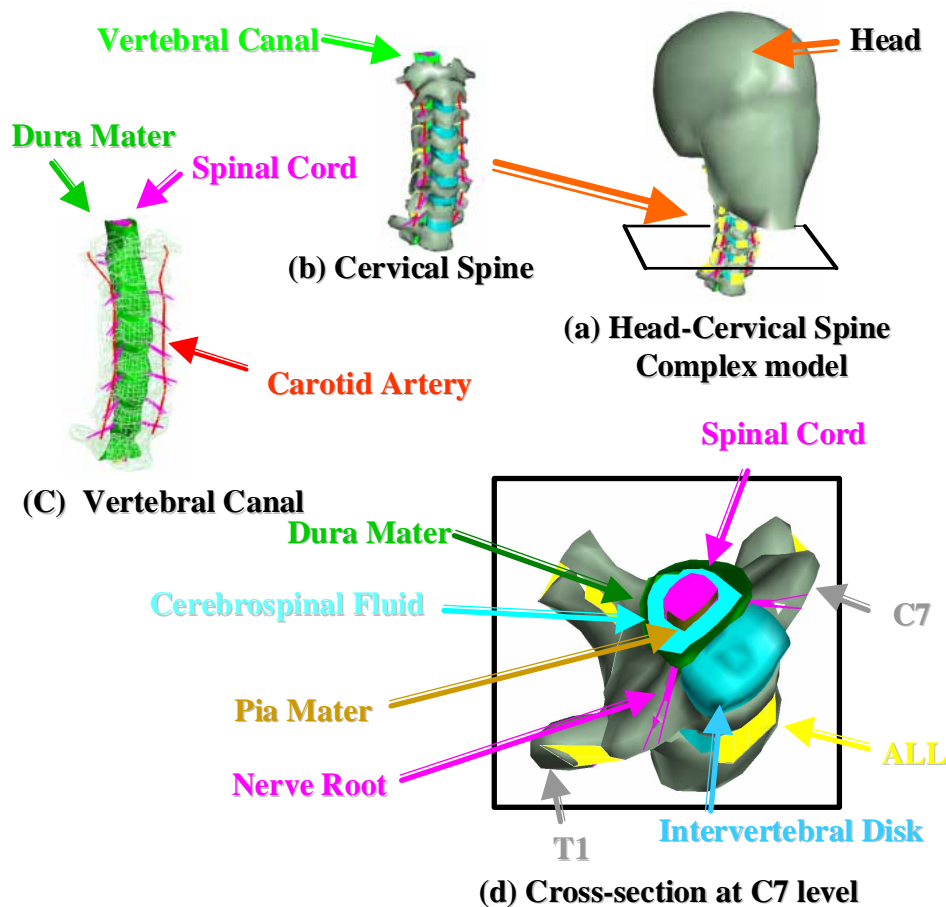


Figure 26 Disassembled Diagrams of the Cervical Spine Model

## Appendix II The sites of whiplash injuries and the failure criterion

Injury sites	Type	Threshold level for criterion	References
Stress on Joint Cartilage	Stress	Shear 5Mpa Compression 25MPa	[18]
Strain on Joint Capsule	Strain	143.6%	[22]
Dura Mater	Strain	Longitudinal 19% Transverse 34.2%	[23]
Nerve	Strain	18.4%	[23]
Artery	Strain	85%	[23]
Intervertebral Disc	Stress	Compression 10.8MPa Tension 3.0MPa	[23]
Neck extensional moment	Moment	57 Nm	
Cortical Bone on vertebral body	Strain	1.5%	[23]
ALL	Strain	36.9%	[22]
PLL	Strain	28.1%	[22]
LF	Strain	88.2%	[22]
ISL	Strain	67.9%	[22]

### Appendix III Material Property

Intervertebral Disc	E=3.57 (MPa)			
Nucleus Eq.(3)	E=2.083 (GPa)	$G_0 = 10.5$ (kPa)	$G_\infty = 0.026$ (kPa)	$\beta = 1200$ (/sec)
Vertebral Body(Cortical Bone)	E=18.9 (GPa)		t=1 (mm)	
Vertebral Body(Spongy Bone)	E=0.162 (GPa)			
Dura Mater (Anterior)	(Longitudinal)E=44.1(MPa)		(Transverse)E=4.668(MPa)	t=0.34 (mm)
Dura Mater (Posterior)	(Longitudinal) E=43.35 (MPa)		(Transverse)E=1.826(MPa)	t=0.69 (mm)
Pia Mater	E=11.5 (MPa)		t=0.069 (mm)	
Spinal Cord Eq. (3)	K=2.19(GPa)	$G_0 = 10$ (kPa)	$G_\infty = 2$ (kPa)	$\beta = 80$ (/sec)
Cerebral-Spinal Fluid Eq.(4)	B=10000 (Pa)	$\gamma = 7$	$P_0 = 0$ (Pa)	
ALL	Reference [21]			
PLL	Reference [21]			
Joint Capsule	Reference [21]			
LF	Reference [21]			
ISL	Reference [21]			
SSL	E=17.1 (MPa)			
Nerve Root	Reference [22]		d=1 (mm)	
Artery	Reference [22]		d=2.5 (mm)	

Where E is Young Modulus, K is Bulk Modulus, G is Shear Modulus, and  $\beta$  is Decay Constant,  
t =Thickness, d = diameter

For linear visco-elastic material,  $G(t) = G_\infty + (G_0 - G_\infty)e^{-\beta t}$  (3)

For the pressure for the Murnaghan Equation of State model,  $P = P_0 + B \left( \left( \frac{\rho}{\rho_0} \right)^\gamma - 1 \right)$  (4)

Where P is pressure,  $P_0$  is initial pressure, and  $\frac{\rho}{\rho_0}$  is the ratio of current mass to the initial mass density and with  $\gamma = 7$ .